cigre Turkey

TEPES
TURKISH JOURNAL OF ELECTRICAL POWER AND ENERGY SYSTEMS

TEPES Vol 1., Issue. 2, 75-83, 2021 **DOI:** 10.5152/tepes.2021.21018

RESEARCH ARTICLE

Design and Control of a PV-FC-BESS-Based Hybrid Renewable Energy System Working in LabVIEW Environment for Short/Long-Duration Irrigation Support in Remote Rural Areas for Paddy Fields

Kumaril Buts, Lillie Dewan, Modi Pandu Ranga Prasad

National Institute of Technology, Kurukshetra, India

Cite this article as: Buts K, Dewan L, Prasad M. Design and control of a PV-FC-BESS-based hybrid renewable energy system working in LabVIEW environment for short/long-duration irrigation support in remote rural areas for paddy fields. *Turk J Electr Power Energy Syst.* 1(2), 75-83, 2021.

ABSTRACT

The reduction of carbon-based energy consumption is one of the critical challenges of the 21st century. The development of efficient and reliable renewable energy is a significant task of this century. Green revolutions boost agriculture and are responsible for a drastic change in grain production, enhancing energy consumption due to optimum use of the agriculture machinery, basically for irrigation purposes. The scope of this paper is to present a Hybrid Renewable Energy System (HRES) that is capable of replacing the diesel pump commonly used for time-bound irrigation, as in the paddy field for rice production. The proposed experimental HRES system consists of a photovoltaic (PV) generator, a fuel cell (FC), and a battery energy storage system (BESS). This system can provide 0.4 kW, single-phase electrical power, tested under varying solar radiation and load demand conditions, suitable for all-weather electrical irrigation pumps of up to 0.5 HP capacity. Controlling of this hybrid system is carried out in the LabVIEW environment.

Index Terms—Battery energy storage system, controlling, hybrid renewable energy system, irrigation pump.

I. INTRODUCTION

Human development is continuous and is directly proportional to the rate of energy consumption. Green energy supply is a forced demand in this present era. Green revolutions boost agriculture and are responsible for a drastic change in grain production, enhancing energy consumption due to optimum use of the agriculture machinery, basically for irrigation purposes. Agriculture is unique because it accounts for 4 to 8 percent of the total energy demand [1] and is susceptible to energy demand. A very famous quote that is often used, is "Everything can wait, but not agriculture", and this quote is highly justified in rice production. On average, about 2500 L of water need to be supplied for a paddy field to produce 1 kg of rough rice (by rainfall and/or irrigation) [2]. During the rice crop's reproductive stage, a water level of a minimum of 10 cm is required to be maintained in the paddy field for at least 20–30 days [3].

Apart from rainwater, farmers are dependent on other irrigation methods. A diesel pump is one of the options for drawing the water from a deep bored well. Diesel pumps are costly and have an adverse impact on the environmental and ecological systems.

A renewable energy-based hybrid system can deliver a constant power supply at the desired load level and can be used to support irrigation. Various renewable energy genres, including wind systems, photovoltaic (PV) cell, fuel cell (FC) (basically hydrogen fuel cell (HFC)), natural gas-based plant, and battery storage system, are well established and enjoy the advantages of matured technology [4].

PV technology is beneficial for places where ample sunshine is available, and grid-support is not available or limited. However, PV-generators are also installed nowadays in grid-tied distribution areas for reducing coal-linked power demand. The power generated by a PV system is highly dependent on the availability of sunny hours. It isn't easy to store the energy generated for future use (i.e., during cloudy days or at night). For reliable operation, other alternate power sources such as FC systems, hydrogen storage tanks, or battery energy storage systems (BESS) must be integrated with a PV system [5,6].

Corresponding author: Kumaril Buts, Kumaril_61900052@nitkkr.ac.in

Received: March 31, 2021
Accepted: May 4, 2021
Published online: August 27, 2021

The HFC is comparatively an old technology which is now at a mature stage. HFC is beneficial for those areas where days of sunshine are less frequent or insufficient to fulfil the continuous load demand. Of the different FC power plants, such as the solid oxide fuel cell (SOFC), molten carbonate fuel cell (MCFC), phosphoric acid fuel cell (PAFC), proton-exchange membrane fuel cell (PEMFC), and others, the PEMFC power plant is preferred. It has been found very suitable, especially for a hybrid energy system [7,8].

Integrating the FC power plant with a battery storage system is economical, rather than using either of them individually. Without a battery system, the FC system must cater to all power demands, which will increase the FC power plant's size and cost, with a reduction in the performance and life due to overloading. The same holds true when the BESS is used alone. In [9], a detailed dynamic model, the design, and simulation of a hybrid energy system have been discussed, with the conclusion that the battery-supported system has some unique features and advantages over systems without battery support.

A PV system for small-scale applications, such as water pumping, street lighting, and irrigation applications in non-grid-supported remote rural areas, is discussed in Sukamongkol and Chungpaibulpatana [10].

A comprehensive technical analysis related to the combined operation of solar PV, wind power, and HFC has been carried out in Zahedi [4], and suggestions have been offered on some technical difficulties regarding the interconnection of hybrid energy sources and their solutions.

Nowadays, control operations performed in the LabVIEW environment are gaining more attention than other software platforms. in Andreadou and Bonavitacola [11], an efficient method for residential load scheduling and control for smart homes in the LabVIEW environment has been presented. PV generator modeling and simulation, working in the LabVIEW platform for small power supply, is presented in Bendib et al. [12]. User-friendly operation and real-time data availability are some of the inherent features of the LabVIEW environment.

A PV, FC, and BESS-based hybrid system is proposed in this paper to irrigate paddy crops. The proposed hybrid system has been simulated in MATLAB/Simulink and implemented on the hardware available in the School of Renewable Energy & Efficiency (SREE) laboratory, NIT, Kurukshetra, India, in the LabVIEW environment, and tested under varying solar radiation and load demand conditions. The combination of FC-BESS with the PV system is an attractive choice due to the high efficiency, fast load–response, cost-effectiveness and reliable operation.

This paper is organized into five sections: after a brief introduction in section 1, and section 2 describes the configuration and behaviour of the elementary components in the proposed system. Section 3 describes the system, and gives a brief idea about the PV-system, FC system, BESS, DC micro-grid, and their controlling techniques, respectively. Section 4 deals with the system's software and hardware development, followed by a conclusion in section 5, and references.

II. PROBLEM STATEMENTS

A comprehensive field study was carried out with the local farmers' help in the southern area of Bihar, a province of India, where paddy is a major food grain produced during the monsoon season. Some parts of this southern zone are hilly, and are not supported by the national grid. From valuable information provided by the paddy farmers, it is concluded that:

1. The rice crop needs approximately 10 mm of water per day.
2. During the rice crop's reproductive time, it is desirable to maintain a water depth at a minimum of 10 cm for at least 20–30 days in the paddy field.

The water requirement of a rice crop is calculated using simple water balance models [3], which include different inflows and outflows of water in a paddy field.

$$ER + I = ET + P + S + SD + CWS \quad (1)$$

where *ER*, effective rainfall; *I*, irrigation supply; *ET*, evapotranspiration loss; *P*, deep percolation loss; *S*, seepage loss; *SD*, surface drainage or run-off loss; and *CWS*, change in water status.

From Equation 1, it is clear that if adequate rainfall is not available, water balance solely depends on irrigation.

By simple calculation, 1 mL of water is required to maintain 10 cm water depth in a 1-ha area of paddy field. The water pump with performance and technical specifications given in Table I will be sufficient, as it will fulfill the water demand within 2–3 hours. Therefore, an irrigation pump of this capacity can be considered ideal for time-bound paddy field irrigation.

Thus, the problem statement is to design a hybrid renewable energy system (RES) comprising PV, FC, and BESS, producing a 0.4 kW continuous supply (day/night & all-weather) to overcome the diesel pump's irrigation cost and adverse environmental impact. This

TABLE I
PERFORMANCE OF A TYPICAL 0.5HP SINGLE-PHASE IRRIGATION WATER PUMP

Specifications	Descriptions
Power rating	0.5 HP (0.37 kW)
Full load current	4 A
Rated voltage	210 V
Water head	4 m
Discharge	15.5 Liters per second (LPS)

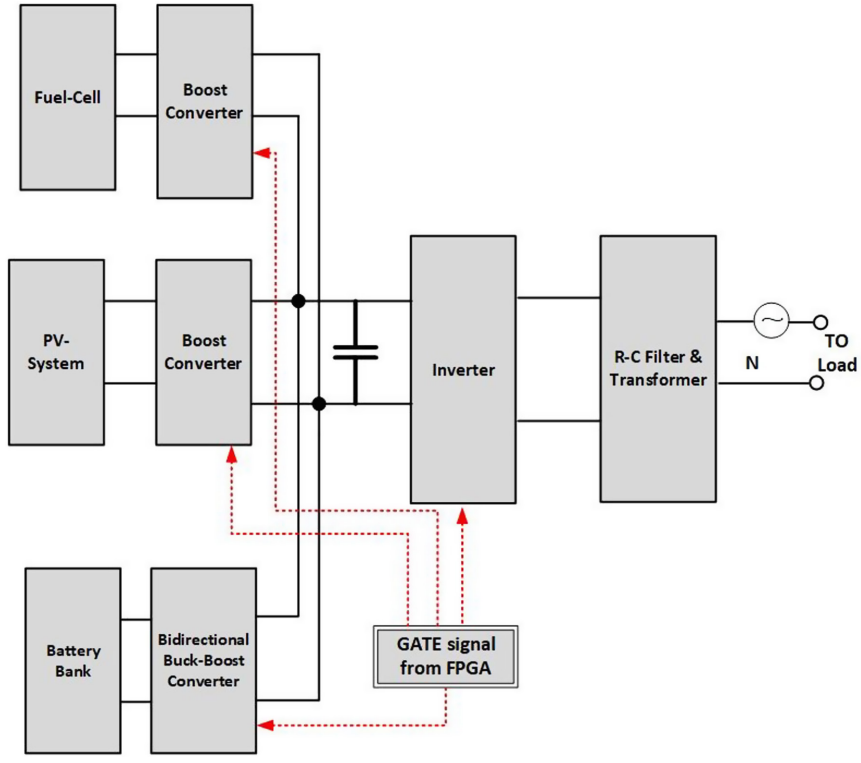

Fig. 1. Line diagram of the hybrid Renewable Energy System (hybrid RES).

system's advantages are that it will be cost-effective, efficient, and reliable for irrigation support, and provide electric power for home illumination when not used for irrigation.

In the next section, a brief description of this hybrid system's components and working is given.

III. SYSTEM DESCRIPTIONS

This proposed hybrid system contains a PV generator, a FC, and a battery system stack. A line diagram of this proposed hybrid system is shown in Fig. 1.

A. The PV System

The illumination of the common junctions between two different materials by photon irradiation, producing electrical potential, is termed a PV effect [13,14]. The electrical characteristics of a PV system can be well illustrated with single- and two-diode models. The single diode model is popular and close to the PV cell's actual behavior [14,15].

Based on the single-diode model, mathematical modeling of the PV system output voltage is expressed as [14],

$$V_{PV} = \frac{N_S nkT}{q} \ln\left[\frac{I_{SC} - I_{PV} + N_P}{N_P I_0}\right] - \frac{N_S}{N_P} R_S I_{PV} \quad (2)$$

where N_S, the number of series cells per string; n, ideality factor; k, Boltzmann constant [J/deg.K]; T, PV cell temperature [deg.K]; q, electronic charge [C]; I_{SC}, short-circuit cell current [A]; I_{PV}, PV cell output current [A]; N_P, the number of parallel strings; I_0, PV cell reverse saturation current [A]; and R_S, series resistance of the PV cell [Ω].

B. The HFC

A FC is an electrochemical device that, like any battery, converts chemical energy into electrical energy [7]. The overall FC is composed of several cells stacked as a single unit [7,15]. An FC power plant uses oxygen and hydrogen as reactants to convert chemical energy into electrical energy.

In the proposed system, mathematical modeling of the HFCs is implemented based on Nernst's instantaneous voltage output equation [7], expressed as:

$$E = N_O\left[E_0 + \frac{RT}{2F}\log\left[\frac{pH_2\sqrt{pO_2}}{pH_2O}\right]\right] \quad (3)$$

where N_O, number of series FCs in the stack; E_0, standard no-load voltage [V]; F, Faraday constant [C/kmol]; R, Universal gas constant [J/kmol K]; T, absolute temperature [K]; pH_2, hydrogen partial pressure [atm]; pH_2O, partial water pressure [atm]; and pO_2, oxygen partial pressure [atm].

C. BESS

A battery is simply an electrochemical cell that produces electrical energy by chemical reactions [16]. A BESS is a stack of cells

connected in series or parallel to provide the desired voltage or current level demand.

The battery voltage, V_{Batt}, is calculated separately by two different equations for the charging and discharging modes [17]. The mathematical modeling of the battery characteristics has been accomplished based on equations 4, 5 & 6 [9,17].

$$V_{Batt(charge)} = V_O - \frac{KQ_{max}}{0.1Q_{max} - q} i^* - \frac{KQ_{max}}{Q_{max} - q} it + A\exp(-Bq) \quad (4)$$

$$V_{Batt(discharge)} = V_O - \frac{KQ_{max}}{Q_{max} - 1} i^* - \frac{KQ_{max}}{Q_{max}} t + A\exp(-Bq) \quad (5)$$

where V_O, constant output voltage of the battery [V]; K, the polarization constant [$(Ah)^{-1}$]; Q_{max}, maximum capacity of the battery [Ah]; i^*, reference current [A]; i, measured (actual) current [A]; q, the available capacity of the battery[Ah]; A, exponential voltage [V]; and B, exponential capacity [$(Ah)^{-1}$].

The state of the charge of the battery (SOC_{Batt}) is calculated as:

$$SOC_{Batt} = 100\left(1 - \frac{\int i(t)\,dt}{Q}\right) \quad (6)$$

where i, instantaneous current [A]; and Q, charge stored [C].

D. DC Micro-Grid

The solar PV system and the HFC act as a DC source and are connected to a DC-link capacitor with a boost converter, while a battery bank also acts as a DC source. It is connected to the DC link via a bidirectional converter.

The voltage source converter (VSC) plays a vital role between the DC-link voltage and the AC loads, acting as a temporary power storage device to provide the voltage source inverter with a steady flow of power. The capacitor's voltage is regulated using a DC-link voltage control loop that balances the capacitor's input and output power. In the proposed hybrid RES system, the VSC controller has a phase-locked loop (PLL) to synchronize the DC power with the load frequency [18,19].

The reference currents and measured currents of the VSC are compared, and are given to relay-based hysteresis controllers. These hysteresis controllers generate the switching logic for the IGBTs of VSC in the manner shown in Table II [20].

E. Power Converters

In this proposed system, the PV generator and the FC output voltage and current are controlled using a boost converter. The pulse width modulation (PWM)-controlling technique is commonly used to control the boost converters and the inverter's output voltage. A full-bridge voltage–source inverter with four IGBT-based power switches is used here for DC to AC power conversion. A bidirectional buck–boost converter is used for charging and discharging of the battery. The output of this bidirectional converter is connected to the inverter through the DC link.

TABLE II
SWITCHING LOGIC OF THE HYSTERESIS CONTROLLER

Switching State	Gate Pulse
I^*_{refA}-$i^*_{measuredA}$> upper band	g_1
I^*_{refA}-$i^*_{measuredA}$< lower band	g_4
I^*_{refB}-$i^*_{measuredB}$> upper band	g_3
I^*_{refB}-$i^*_{measuredB}$< lower band	g_2

F. Field-Programmable Gate Array

A field-programmable gate array (FPGA) provides the most convenient way of designing the PWM generator for power converters. FPGAs are like a digital circuit that can be electrically coded to obtain the required modulation signals [21].

In this proposed system, an FPGA-based micro-controller chip is used for generating and controlling the gate pulses with the help of Very High-Speed Integrated Chip Hardware Description Language (VHDL) physical architecture. The VHDL code for the PWM generator is written using the Xilinx ISE 10.1software.

IV. IMPLEMENTATION

The proposed hybrid system is simulated on MATLAB/Simulink2017A and then implemented on the hardware available in the laboratory of SREE, NIT Kurukshetra, India, in the LabVIEW2018environment.

This hybrid system consists of five components: the PV generator, the FC, the BESS system, power converters with specifications given in Table III, and the control section.

The PV system based on four mono-crystalline modules connected in series can generate up to 1 kW. Each module can generate 250 W of peak power. Rating of the PV generator chosen is based on exploiting its maximum benefit within the economic boundary.

The maximum power output of the HFC with a total of 48 cells connected in series is up to 1 kW.

The BESS consists of 12 Li-ion battery units connected in series. The total output capacity of the BESS system is up to 1 kW. The RL load of 0.4 kW active power-drawing capacity equivalent to the load of the desired irrigation pump capacity has been used to verify the performance of the proposed HRES.

A. MATLAB Implementation

The MATLAB Simulation arrangement, as shown in Fig. 2, is developed based on the mathematical modeling, equations from (2) to (6), and the line diagram of the system as shown in Fig. 1. Rating of the components in MATLAB is taken precisely, like that of the hardware setup.

TABLE III
RATINGS OF THE COMPONENTS OF THE HARDWARE SETUP

Field-Programmable Gate Array (FPGA) Box		
1.	Control card technology	FPGA
2.	Pull-up card for inverter gate firing	8 Pulse-Width Modulation (PWM) signals
Single-phase inverter		
1.	Maximum DC input voltage	150 V
2.	Output voltage	100 V AC
3.	Output current	5 A
4.	Switching frequency	10 kHz
LC filter for the single-phase inverter		
1.	Inductor	3 mH, 10A
2.	Capacitor	10 µF
PhotoVoltaic (PV) system specifications and ratings		
1.	Number of channels	2
2.	Short-circuit current per channel	0–20 A
3.	Open-circuit voltage per channel	0–50 V DC
4.	Maximum output power per channel	500 W
Boost converter for PV system		
1.	Input voltage	50 V
2.	Input current	20 A
3.	Output voltage	150 V
4.	Output current	10 A
5.	Switching frequency	20 kHz
Fuel cell components		
1.	Type of the fuel cell	Proton Exchange Membrane (PEM)
2.	Number of cells	48
3.	Rated power	1000 W
4.	Performance	28.8 V and 35 A
5.	Reactants	Hydrogen and air
6.	Maximum stack temperature	65°C
7.	Flow rate at maximum output	13 Liters per minute
Boost converter for fuel cell		
1.	Input voltage	28.8 V at full load
2.	Input current	35 A at full load
3.	Output voltage	150 V
4.	Output current	10 A
5.	Switching frequency	20 kHz
Battery energy storage system (BESS)		
1.	Battery type	Lead-acid
2.	Number of batteries	8, connected in series
3.	Overall output voltage	96 V
4.	Overall capacity	26 Ah
Bidirectional buck-boost converter for BESS		
1.	Input voltage	105 V (battery side)
2.	Output voltage	150 V (inverter side)
3.	Output current	10 A
4.	Switching frequency	20 kHz

B. Hardware Implementation

Based on the MATLAB model, hardware implementation is carried out in the laboratory, under varying solar radiation and load demand conditions, as shown in Fig. 3. The solar radiation and power demand data are based on real-world records.

Controlling the hardware components is carried out in the LabVIEW environment, and a simplified and user-friendly control panel is developed. A personal computer (PC) and an FPGA-based micro-controller placed in the hardware setup communicate with a LAN/ethernet cable.

C. Results and Discussions

The real-time data obtained from the hardware setup with a LabVIEW-based data analyzer and data stored in the Excel sheet is plotted with the help of the graph-plotter.

For power storage or to mitigate the load demands, the battery is operated in charging/discharging mode. Output voltage and current with frequency are captured on a real-time power analyzer (HIOKI 3360 series) during the battery charging and discharging time, respectively.

Comparative analyses (quantitative and qualitative) of the MATLAB simulation and the hardware results, as shown in Fig. 4 and 5, summarized in Table IV, provide the following important information:

- Battery charging/discharging activity during the load change is fast and responsive.
- The system is stable and fulfills the desired load demands.
- Frequency remains within the limit with ± 5% tolerance, which is acceptable.

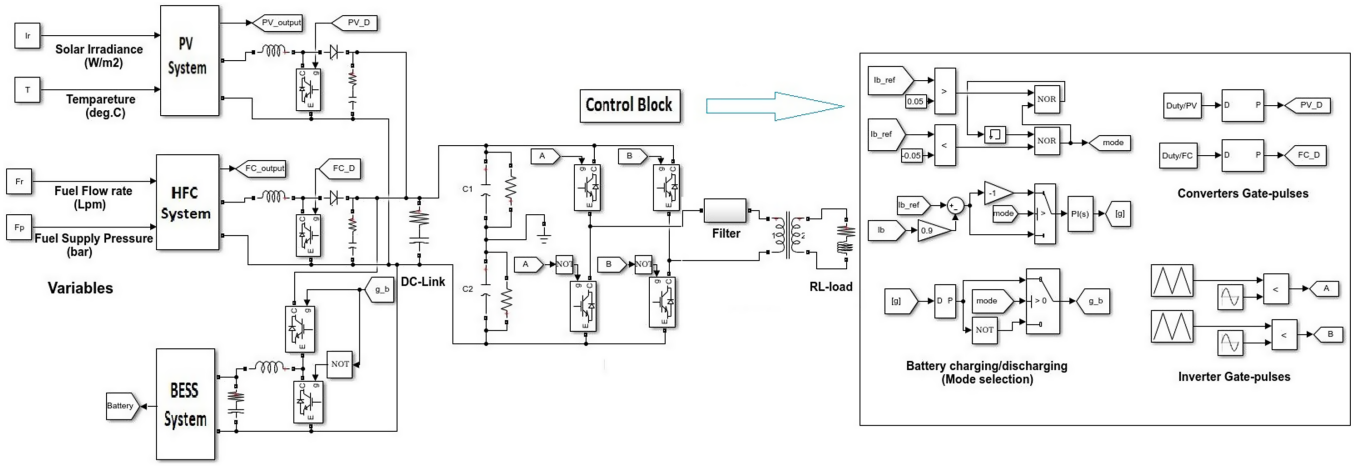

Fig. 2. Simulation arrangement of the hybrid Renewable Energy System.

- MATLAB model of the system mimics the behavior of the actual hardware setup. It can be said that desired system can generate sufficient power to run the irrigation pump.
- From Table IV, it has been observed that the performance of the battery in HRES has good transient and steady-state characteristics.
- The limitation in the system designed is that it provides a limited load demand. However, the design can be expanded to mitigate the higher load by changing the components' rating. During the off-irrigation period, the proposed HRES system can illuminate farms and homes.

V. CONCLUSION

The PV/FC/BESS hybrid power system designed and modeled for irrigation purposes is suitable not only for paddy fields but also for any crop. This hybrid system works in a standalone mode with controlling activity in the LabVIEW environment.

The hybrid system's dynamic behaviors have been tested under varying solar radiation and load demand conditions, where the solar radiation and power demand data are based on real-world records. The LabVIEW-based control strategy for the developed system is efficient and exhibits excellent performance, even for extended periods.

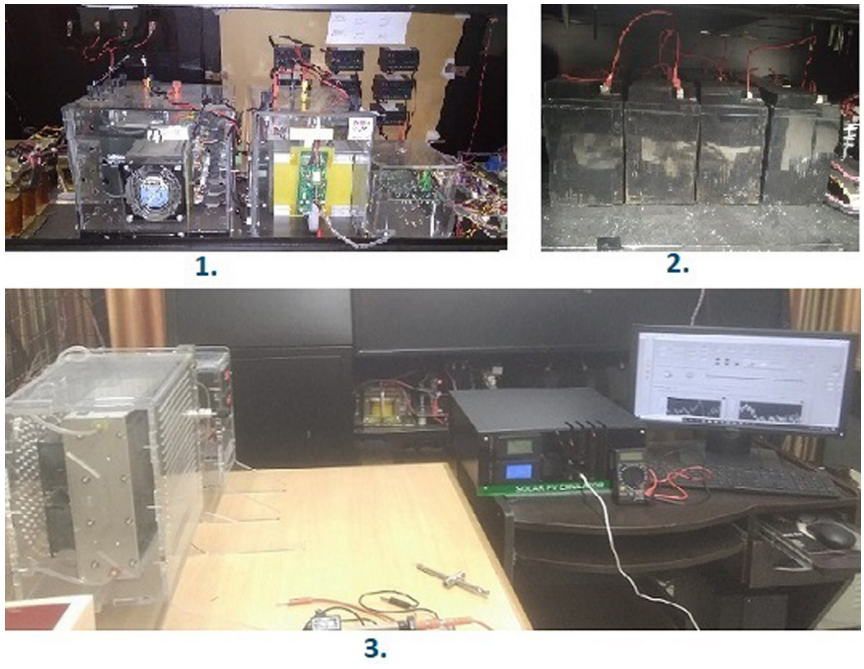

Fig. 3. Hardware setup of the hybrid Renewable Energy System in the lab (a) Converters and inverter setup; (b) Battery stack; and (c) FC & PV emulator connected with the system).

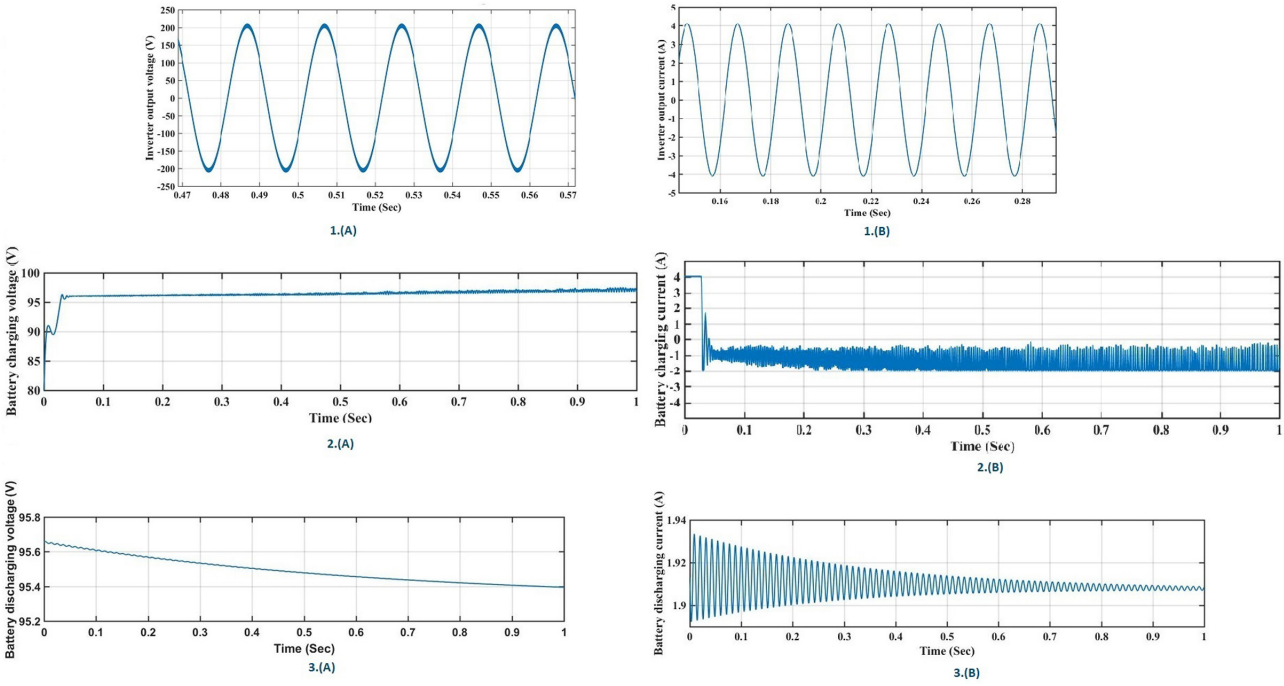

Fig. 4. Simulation results of the MATLAB model of the hybrid Renewable Energy System (1(a) and 1(b): Inverter voltage and current output; 2(a) and 2(b) Battery voltage and current during charging; and 3(a) and 3(b) Battery voltage and current during discharging).

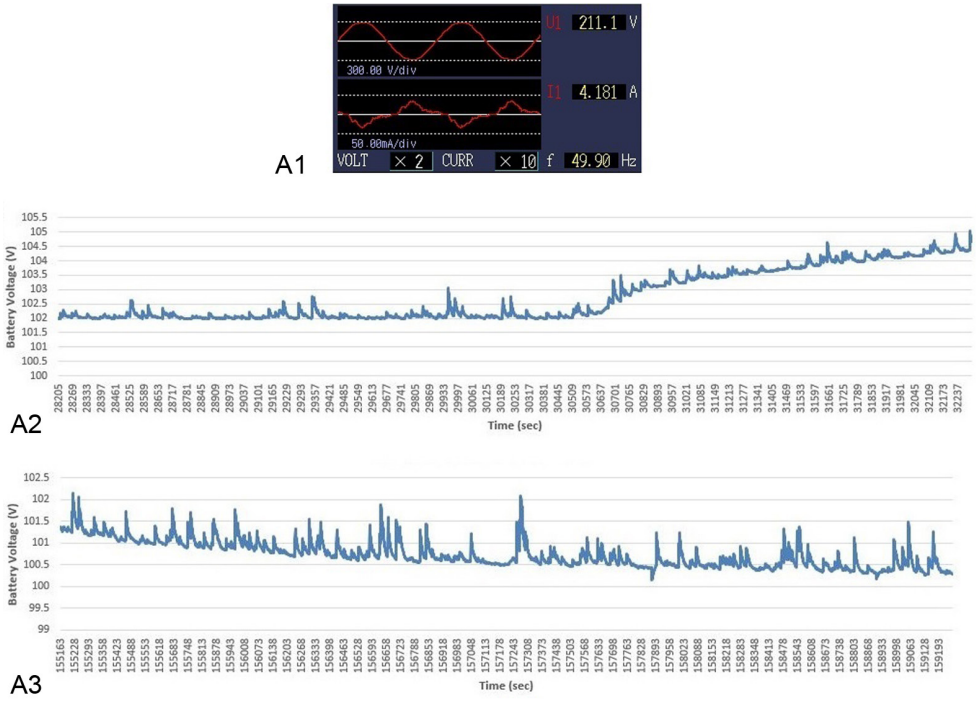

Fig. 5. Results from the hardware setup of the hybrid Renewable Energy System (1(a) and 1(b) Output voltage, current, and frequency from the load-side during charging and discharging of the battery; 2(a) and 2(b) Battery voltage and current during charging; and 3(a) and 3(b) Battery voltage and current during discharging).

Fig. 5. (*Continued*) Results from the hardware setup of the hybrid Renewable Energy System (1(a) and 1(b) Output voltage, current, and frequency from the load-side during charging and discharging of the battery; 2(a) and 2(b) Battery voltage and current during charging; and 3(a) and 3(b) Battery voltage and current during discharging).

TABLE IV
STEP RESPONSE CHARACTERISTICS OF THE BATTERY CURRENT SIGNALS

Battery Current During Charging		
	Simulation Results	Hardware Results
Rise time (s)	0.271	0.001
Settling time (s)	0.738	0.001
Overshoot	0.03	0
Undershoot	2.1	0
Peak (A)	0.87	1
Battery current during discharging		
	Simulation Results	Hardware Results
Rise time (s)	0.181	0.001
Settling time (s)	0.98	0.001
Overshoot	1.935	0
Undershoot	0.88	0
Peak (A)	1.94	2

Peer-review: Externally peer-reviewed.

Conflict of Interest: The authors have no conflicts of interest to declare.

Financial Disclosure: The authors declared that this study has received no financial support.

Acknowledgment: The hardware implementation was carried out in the School of Renewable Energy and Efficiency (SREE) Lab, NIT, Kurukshetra, India. Thanks to the coordinator, SREE, for providing this opportunity.

REFERENCES

1. Food and Agriculture Organisation, "Annual report on agriculture-2020," related resources. [online] Available: https://www.fao.org. chapter 2: *Energy_for_Agriculture*.
2. Bas Bouman, *Rice Today*. Philippines: International Rice Research Institute, IRRI, Tech. Rep. Jan-Mar issue, vol. 12, no. 1, pp. 38–45, 2009.
3. S. Aryal, "Rainfall and water requirement of rice during growing period," *Journal of Agriculture and Environment*, vol. 13, 2012.
4. A. Zahedi, "Technical analysis of an electric power system consisting of solar PV energy, wind power, and hydrogen fuel cell," in *2007 Australasian Universities Power Engineering Conference*, Perth, WA, Australia, December 09-12, 2007, pp. 1–5. [CrossRef]
5. T. F. El-Shatter and M. N. Eskandar, "Hybrid PV/fuel cell system design and simulation," *Renewable Energy*, vol. 27, no. 3, pp. 479–485, 2002.
6. G. Barchi, G. Miori, D. Moser, and S. Papantoniou, "A small-scale prototype for the optimization of PV generation and battery storage through

the use of a building energy management system," in *2018 IEEE International Conference on Environment and Electrical Engineering and 2018 IEEE Industrial and Commercial Power Systems Europe (EEEIC / I&CPS Europe)*, 2018, pp. 1–5. (doi: 10.1109/EEEIC.2018.8494012)

7. T. Zhou and B. Francois, "Modeling and control design of hydrogen production process for an active hydrogen/wind hybrid power system," *International Journal of Hydrogen Energy*, vol. 34, pp. 21–30, 2009. June 05, 2014.
8. H. Gorgun, "Dynamic modeling of a proton exchange membrane (PEM) electrolyzer," *International Journal of Hydrogen Energy*, vol. 31, no. 1, pp. 29–38, 2006. September, 2018.
9. K. Buts, L. Dewan, and M. P. R. Prasad, "Modeling and implementation of wind-battery storage hybrid power system in LabVIEW environment," in *1st IEEE Conference ICMICA*. NITK, 2020, pp. 1–6. (doi: 10.1109/ICMICA48462.2020.9242826)
10. Y. Sukamongkol and A. Chungpaibulpatana, "A simulation model for predicting the performance of a solar photovoltaic system with alternating current loads," *Renewable Energy*, February 06, 2007, vol. 27, no. 2, pp. 237–58, 2007.
11. N. Andreadou and F. Bonavitacola, "Residential remote load scheduling and control for smart homes with LabVIEW interface," in *IEEE International Conference on Communications, Control, and Computing Technologies for Smart Grids (SmartGridComm)*, Aalborg, Denmark, October 29-31, 2018 February 06, 2007, 2018, pp. 1–7. [CrossRef]
12. B. Bendib, H. Belmili, S. Boulouma, H. Rahmani, and F. Krim, "Modeling and simulation of PV generator characteristics under LabVIEW," In *2018 6th International Renewable and Sustainable Energy Conference (IRSEC)*, Rabat, Morocco, December 05-08, 2018, 2018, pp. 1–6. [CrossRef]
13. R. Luthander and J. Widen, "Photovoltaic self consumption in Buildings: A review," *Applied Energy*, vol. 142, pp. 80–94, January 12, 2015.
14. M. Uzunoglu and O.C. Onar, "Modeling, control and simulation of a PV/FC/UC based hybrid power generation system for stand-alone applications," *Elsevier, Science Direct*, *Renewable Energy*, July 25, 2008, vol. 34, pp. 509–520, 2009.
15. K. Rajashekara, "Hybrid fuel-cell strategies for clean power generation," *IEEE Transactions on Industry Applications*, vol. 41, no. 3, pp. 682–689, 2005. [CrossRef]
16. T. Wei *et al.*, "Battery management and application for energy-efficient buildings," in *2014 51st ACM/EDAC/IEEE Design Automation Conference (DAC)*, June 05, 2014, pp. 1–6. [CrossRef]
17. F. Fan, N. Tai, X. Zheng, W. Huang, and J. Shi, "Equalization strategy for multi-battery energy storage systems using maximum consistency tracking algorithm of the conditional depreciation," *IEEE Transactions on Energy Conversion*, September 2018. vol. 33, no. 3, pp. 1242–1254, 2018. [CrossRef]
18. V. Tipsuwanporn, A. Charoen, A. Numsomran, and K. Phipek, "A single-phase PWM inverter controlling base on PLL technique," in *SICE Annual Conference*, 2011, pp. 1178–1183.
19. Q. Zhang, X. Sun, Y. Zhong, M. Matsui, and B. Ren, "Analysis and design of a digital phase-locked loop for single-phase grid-connected power conversion systems," *IEEE Transactions on Industrial Electronics*, vol. 58, no. 8, pp. 3581–3592, 2011. (doi: 10.1109/TIE.2010.2087295)
20. H. Mao, X. Yang, Z. Chen, and Z. Wang, "A hysteresis current controller for single-phase three-level voltage source inverters," *IEEE Transactions on Power Electronics*, January 02, 2012, vol. 27, no. 7, pp. 3330–3339, 2012. [CrossRef]
21. F. Umer and M. Zied, *Tree-based Heterogeneous FPGA Architectures*. Rabat, Morocco, December 05-08, 2018, Springer, 2012, pp. 8–47.